Materials Today: Proceedings xxx (xxxx) xxx

Contents lists available at ScienceDirect

Materials Today: Proceedings

journal homepage: www.elsevier.com/locate/matpr

Effect of Mg on structural, morphological and optical properties of Mg-doped V_2O_5 nanostructures

Sandesh kumar Rai [a,b,*], Rajesh Rai [c], Raghavendra Bairy [d], Vijeth H. [e], Jayarama A. [f]

[a] Department of Mechanical Engineering, Canara Engineering College, Mangalore 574219, India
[b] Regional Research Center, Visvesvaraya Technological University, Belagavi 590 018, India
[c] Department of Mechanical Engineering, AJIET, Mangalore 575006, India
[d] Department of Physics, NMAM Institute of Technology (Visvesvaraya Technological University, Belagavi), Nitte, Karkala 574110, India
[e] Department of Physics, Dr.NSAM First Grade College, Nitte, Karkala 574110, India
[f] Department of Physics, Alvas Institute of Engineering & Technology, Moodbidri 574225, India

ARTICLE INFO

Article history:
Received 16 December 2020
Accepted 11 January 2021
Available online xxxx

Keywords:
Mg-doped V_2O_5
Spray pyrolysis
XRD
Surface morphology
AFM
Optical properties

ABSTRACT

The spray pyrolysis is the simple and most promising thin-film fabrication technique in the deposition of Vanadium pentoxide (V_2O_5) thin film. Thin films of pure V_2O_5 and Magnesium (Mg) doped V_2O_5 were fabricated by spraying precursor solution on a glass substrate by spray pyrolysis at 350 °C. The doping concentrations of 1, 3, 5, & 10 wt% of Mg deposited followed by the heat treatment process at 350 °C. Field emission scanning microscopy (FESEM) and atomic force microscope (AFM) images have been used to study the morphology of the film showed the presence of white nanoparticles and surface roughness thereby effect of doping have been noticed. The XRD study shows the increase in the growth of film in (200) direction and enhancement in crystallite size with increase in doping. EDAX study confirms the presence of vanadium and doped Magnesium. Optical property study using UV–visible spectroscopy shows a rapid decrease in absorbance whereas transmittance increases with an increase in wavelength and also observed varying optical bandgap (Eg) from 3.55 eV to 3.75 eV for pure and Mg-doped V_2O_5 thin films. Compared to other transition metals, V_2O_5 exhibits properties appropriate for lithium-ion batteries and sensor applications at very low Mg-doping concentrations.

Selection and peer-review under responsibility of the scientific committee of the International Conference on Smart and Sustainable Developments in Materials, Manufacturing and Energy Engineering.

1. Introduction

Due to the outstanding inclusive and physiochemical properties, advancement in nanomaterials especially on transition metal oxides such as V_2O_5 has gained considerable attention nowadays [1–4]. The V_2O_5 based devices are suitable for UV detectors, switching devices, catalysts, sensors, field-effect transistors, piezoelectric devices, storage medium, electro-optical devices, hydrogen storage, etc. due to its properties like n-type conductivity, high specific power, electrical resistivity, transmission, variable oxidation states, magnetic susceptibility, high energy density [5–14].

Latest researches on V_2O_5 thin films reports various oxidation states of vanadium ions of V_2O_5 that controls defects by forming a useful oxide surface and sensing gas through chemisorption [15–18]. It has been reported that the high Mg content in V_2O_5 thin films found to be more suitable for high colouration efficiency, high visible transmittance, fast switching response time and electrochromic windows. Superior or at least comparable characteristics have been identified for V_2O_5doped with other transition metal films like Mg-doped films [19]. Current research is focused on the physical properties of Magnesium (Mg) doped with V_2O_5-nano structures prepared by spray pyrolysis for device applications.

The thin film deposition methods are mainly classified into chemical and physical deposition techniques. The physical method includes molecular beam epitaxy (MBE), vacuum evaporation, laser ablation and sputtering [20]. The chemical deposition technique includes solution and gas phase-based technique. It is simple, easy and makes use of precursors. Spray pyrolysis, Spin coating, sol–gel and dip coating are some of the solution-based methods [21–23].

* Corresponding author at: Department of Mechanical Engineering, Canara Engineering College, Mangalore 574219, India.
E-mail address: sandeshkumarrai@canaraengineering.in (S. kumar Rai).

https://doi.org/10.1016/j.matpr.2021.01.304
2214-7853/
Selection and peer-review under responsibility of the scientific committee of the International Conference on Smart and Sustainable Developments in Materials, Manufacturing and Energy Engineering.

Gas-based techniques include chemical vapour deposition (CVD), atomic layer deposition etc. The choice of deposition method is usually based on the suitability of the technique for the material used, the degree of deposition control and the costs of deposition.

Spray pyrolysis is found to be a very convenient method to deposit V_2O_5 thin films as wide areas can be easily grown with high growth rates, low cost and minimal waste. In recent years, the spray pyrolysis method has been adopted to integrate dopant ions into semiconductor materials; this provides an easy way to replace elements within desired percentage through precursor solution. It is well reported that gas sensor's sensitivity and selectivity depends upon the surface morphology of the thin film and shift in resistivity as the gas comes into contact with the oxide layer; both depend primarily on the film's crystallite or grain size [24]. Considering the above parameters spray pyrolysis method found to be more suitable for V_2O_5 based thin film deposition.

2. Experimental

2.1. Sample preparation

The pure V_2O_5 and Mg-doped V_2O_5 was deposited by spray pyrolysis on glass substrates with different dopant percentages of thin films. The precursor solution was prepared by adding a few drops of concentrated HCl to the ammonium metavanadate in 100 ml of distilled water at a concentration of 0.02 M. The Mg doping carried by adding concentrations of 0,1,3,5,10 and 20 wt% of Magnesium chloride ($MgCl_2$) to the V_2O_5 precursor solution. The prepared solution is directly sprayed at the substrate temperature of 350 °C onto the well-cleaned glass substrate [25]. For the thin films, the deposition conditions using spray pyrolysis are given in Table 1. The estimated thickness of ~ 200 nm films were prepared and kept in a hot air oven at 350° C for about one hour annealing to evaporate the organic residuals present in the solutions.

2.2. Characterizations of material

The pure V_2O_5 and Mg-doped V_2O_5 thin films thickness were calculated using sensitive microbalance by gravimetric weight difference method. The film samples were assumed to be uniform throughout. An approximate 200 nm thick films were prepared. The Bruker's XRD source used for structural properties study has been carried by adjusting the diffraction angle 2θ with a wavelength of 1.5406 Å. The grain size of the particle in the film is analysed by FESEM images. The film composition using EDAX and surface roughness of films by AFM images help in elementary investigation of the films. The percentage elemental composition using EDAX is tabulated in Table 2. The optical parameters like optical bandgap(Eg), absorption coefficient and transmittance were calculated using UV–visible double-beam spectrophotometer.

Table 1
Spray pyrolysis parameters for the deposition of Mg doped V_2O_5 thin films.

Spray Parameters	Optimum Values
Substrate temperature	350 °C
Ammonium metavanadate solution concentration	0.02 M
Magnesium chloride solution concentration	0.02 M
Solvent	Deionised water
Volume % of Mg	1, 3, 5, 10 and 20
Carrier air Pressure	2 bars
Substrate to nozzle distance	24 cm
Solution spray rate	1 ml/min
Nozzle diameter	0.8 mm
Spray Duration	≈10 mins

Table 2
Atomic percentage of functional material using EDAX.

Elements	Pure V_2O_5	1% Mg	3% Mg	5% Mg	10% Mg
O	50.23	50.13	49.45	50.16	50.29
V	49.77	48.76	47.31	44.86	39.95
Mg	0	1.11	3.24	4.98	9.76

3. Results and discussions

3.1. Analysis of structural properties by XRD study

The X-ray Diffractometer (XRD) data collected using a Rigaku powder X-ray diffractometer equipped with Cu Kα radiation (k = 1.5406 Å) through the range from 10° to 75° help in assessing the crystallite structural properties of the thin film. Fig. 1 shows the diffraction patterns of pure and Mg-doped V_2O_5 thin films. The diffraction pattern of pure V_2O_5 is well-matched with standard V_2O_5 diffraction pattern [26]. The observation from graphs shows increase in concentration of Mg doping increases the intensity of the diffraction peaks. For the different concentrations of Mg doping, the diffraction peak with minimal change is observed. At the diffraction angle (2θ) = 12.28° the XRD patterns corresponding to the plane (200) suggests that the films formed are polycrystalline and crystallised under the orthorhombic structure. XRD spectra indicate that the size of crystallite increases with dopant concentration.

The Scherrer equation [27] is used calculate the crystallite size based on the width of (200) peak, which is obtained at ~ 12.28 on a 2θ scale.

$$D_{avg} = \frac{0.9\lambda}{\beta \cos\theta} \quad (1)$$

where D_{avg} is the crystallite size, θ is the Bragg's angle and β is the full width at half maximum (FWHM) in radians. The Mg doped V_2O_5 XRD peaks show that the crystal structure of V_2O_5 is well established after replacing with Mg. The determined values of lattice constants a and c [28] and the interplanar spacing d_{hkl} using the formula (2) are tabulated in Table 3.

$$\frac{1}{(d_{hkl})^2} = \frac{4(h^2 + hk + k^2)}{3a^2} + \frac{l^2}{c^2} \quad (2)$$

Where *h, k* and *l* are the miller indices $d_{hkl}$is the inter planar spacing, a and c are lattice constants. The value of lattice constant a and c increase with the increase in concentration up to 3% doping

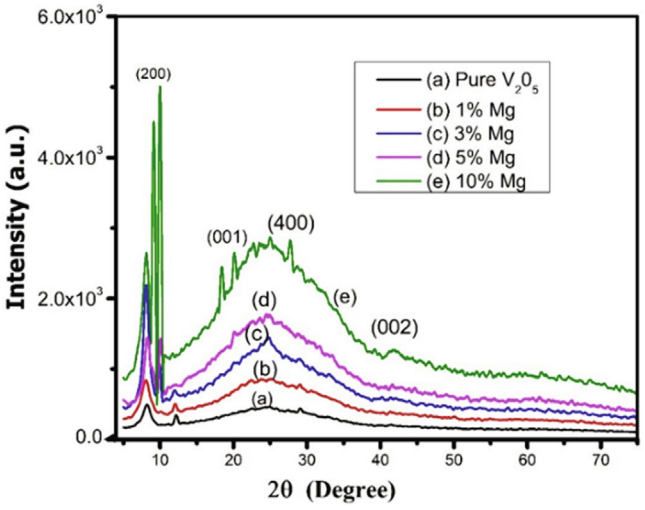

Fig. 1. V_2O_5 and Mg-doped V_2O_5 thin films XRD patterns.

Table 3
XRD structural parameter of Mg doped V_2O_5.

Sample % wt Mg	2θ(Degrees)	FWHM(Degrees)	$D_{avg}(A)$	Lattice parameters (A)		$d_{(hkl)}(A)$
				a	c	
Pure V_2O_5	8.34	19.4595	4.09167	14.68402	21.17803	5.45113
1% Mg	8.28	18.45292	4.3147	14.79024	21.33122	5.49056
3% Mg	7.97	24.87438	3.20024	15.34916	22.13731	5.69805
5% Mg	8.3	19.5922	4.06385	14.75466	21.27991	5.47735
10% Mg	9.98	24.24857	3.28734	12.2757	17.70463	4.55709

and with further increase in doping would decreases the lattice parameters, whereas, ratio of c/a remains constant as ~ 1.44. It is observed that doping with Mg increases the crystallite dimensions of the films.

3.2. Morphological properties

Microscopic features of pure and Mg-doped thin films have been studied using FESEM images. Fig. 2(a-e) shows FESEM images

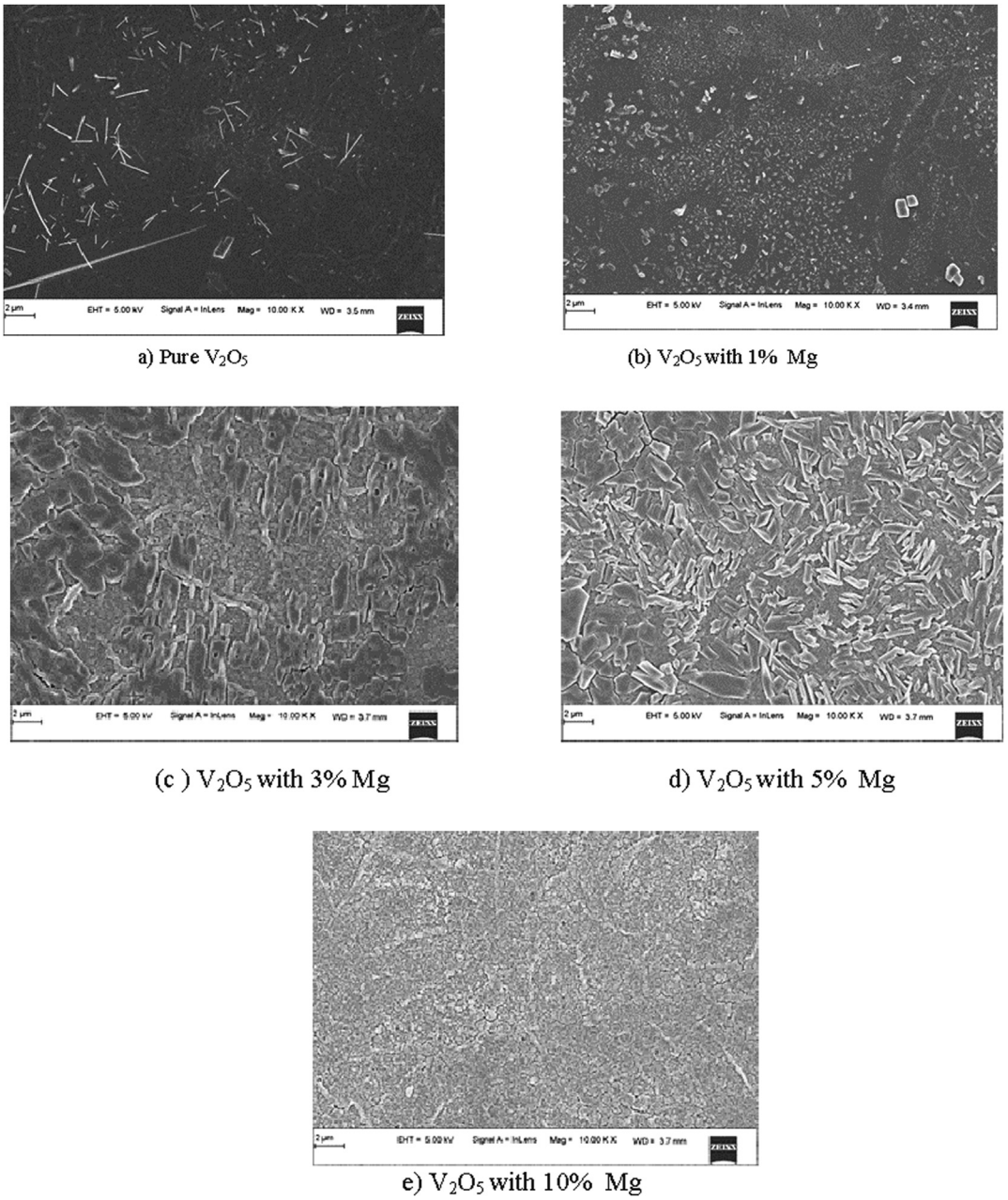

Fig. 2. FESEM images of: a) pure V_2O_5, b) 1%, c) 3%, d) 5%, and e) 10% Mg-doped V_2O_5 thin films.

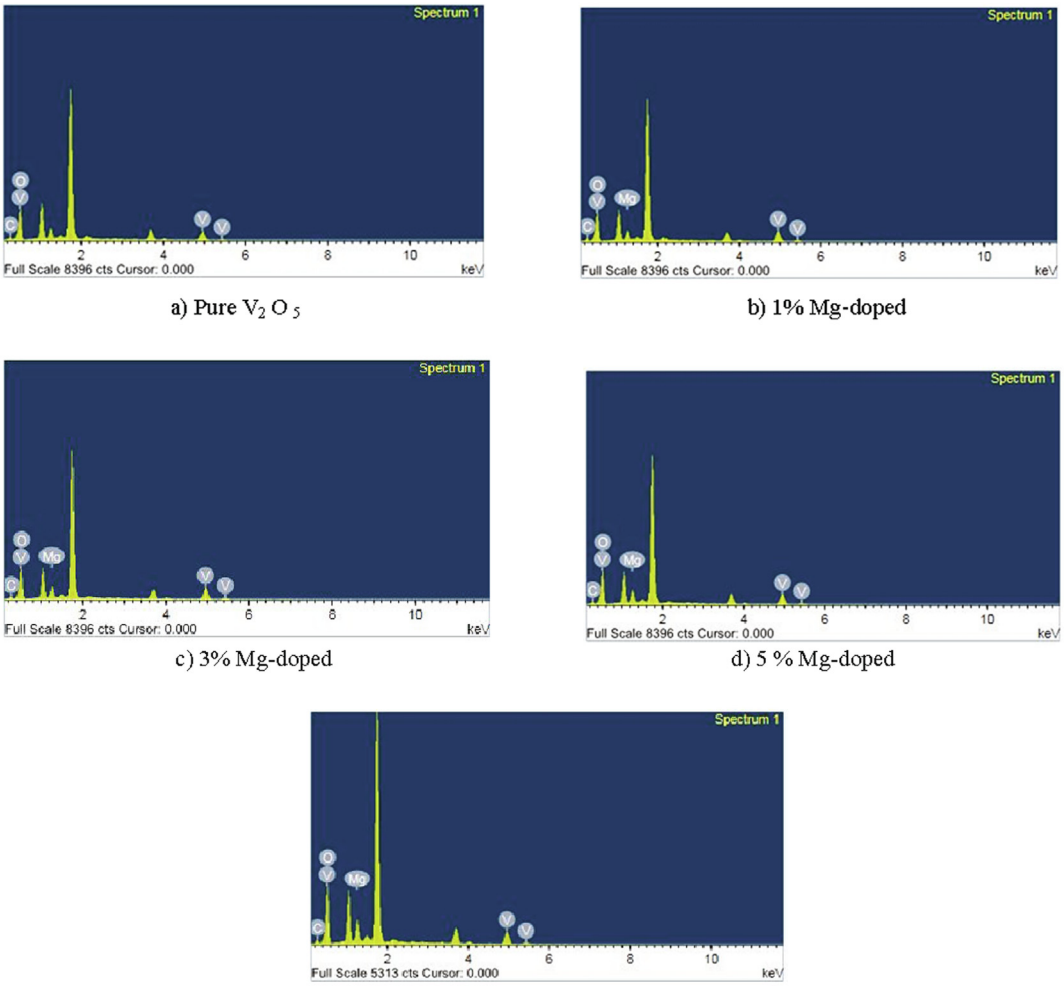

Fig 3. (a-e) EDAX spectrum of Mg-doped V_2O_5 thin films.

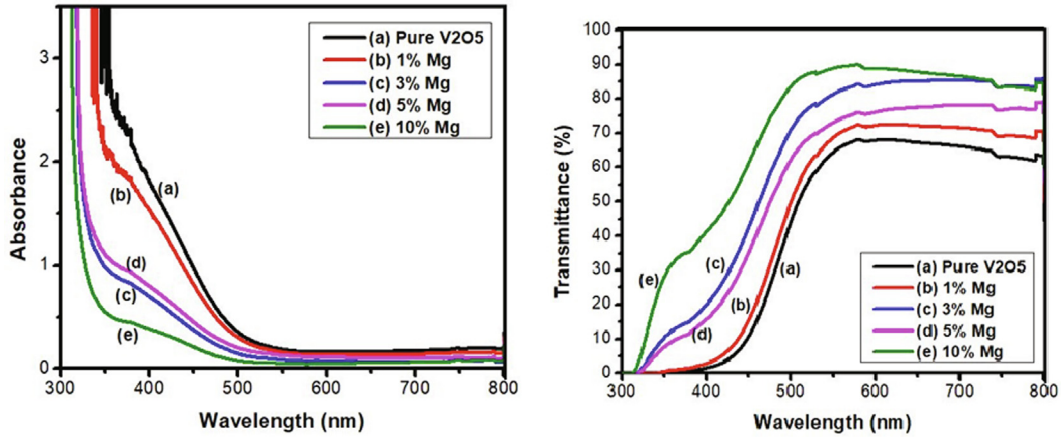

Fig. 4. (a): Absorbance Vs Wavelength for pure and Mg doped V_2O_5 films (b): Transmittance Vs Wavelength for pure and Mg doped V_2O_5 films.

of pure V_2O_5 and Mg-doped with V_2O_5 thin films. A uniform structures are observed for the undoped film. With Mg integration, the structure transforms into the randomly scattered small rock-like white structure and in 3% doping image shows rod-like structures. Further increase in dopant (5%) shows an increase in the size of these rods. But for the 10% dopant, the uniform crystalline structure throughout was observed. Nevertheless, the dopant (Mg) concentration raises the grain sizes of the films. The nanoparticles average sizes are 40–100 nm and were found in a spherical shape. The Energy dispersive X-ray (EDAX) spectrum images in Fig. 3.

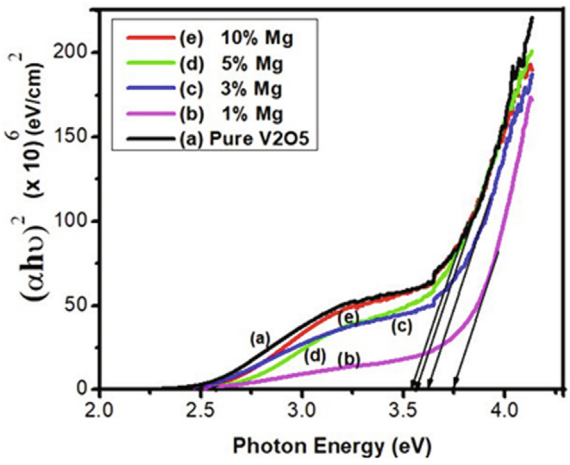

Fig. 5. Plot of $\alpha h\upsilon^2$ vs photon energy for pure and Mg doped V_2O_5 films.

show predicted elements like V, O and Mg in the elementary composition of the prepared thin films of pure V_2O_5 and Mg-doped films.

3.3. Optical properties

UV–Visible double-beam spectrophotometer investigates electronic transitions using optical absorption spectra for undoped and doped V_2O_5 thin films in the range of 300 nm –800 nm is as shown in Fig. 4(a) and (b). The figure indicates a fast decline in absorption with wavelengths corresponding to the prepared thin - film bandgap while transmittance increases with wavelength. The tauc plot [29] determines the optical direct energy band-gap (E_g) for the thin film prepared and is shown in Fig. 5. The energy band gap found between 3.53 eV and 3.75 eV in V_2O_5 thin films for 0 to 10% of Mg concentrations as shown. The Eg for pure V_2O_5 is found to be 3.53 eV. It is noticed that the E_g value increases to 3.75 eV with 1 wt% doping (Mg) concentration and will keep decreasing with increased Mg doping.

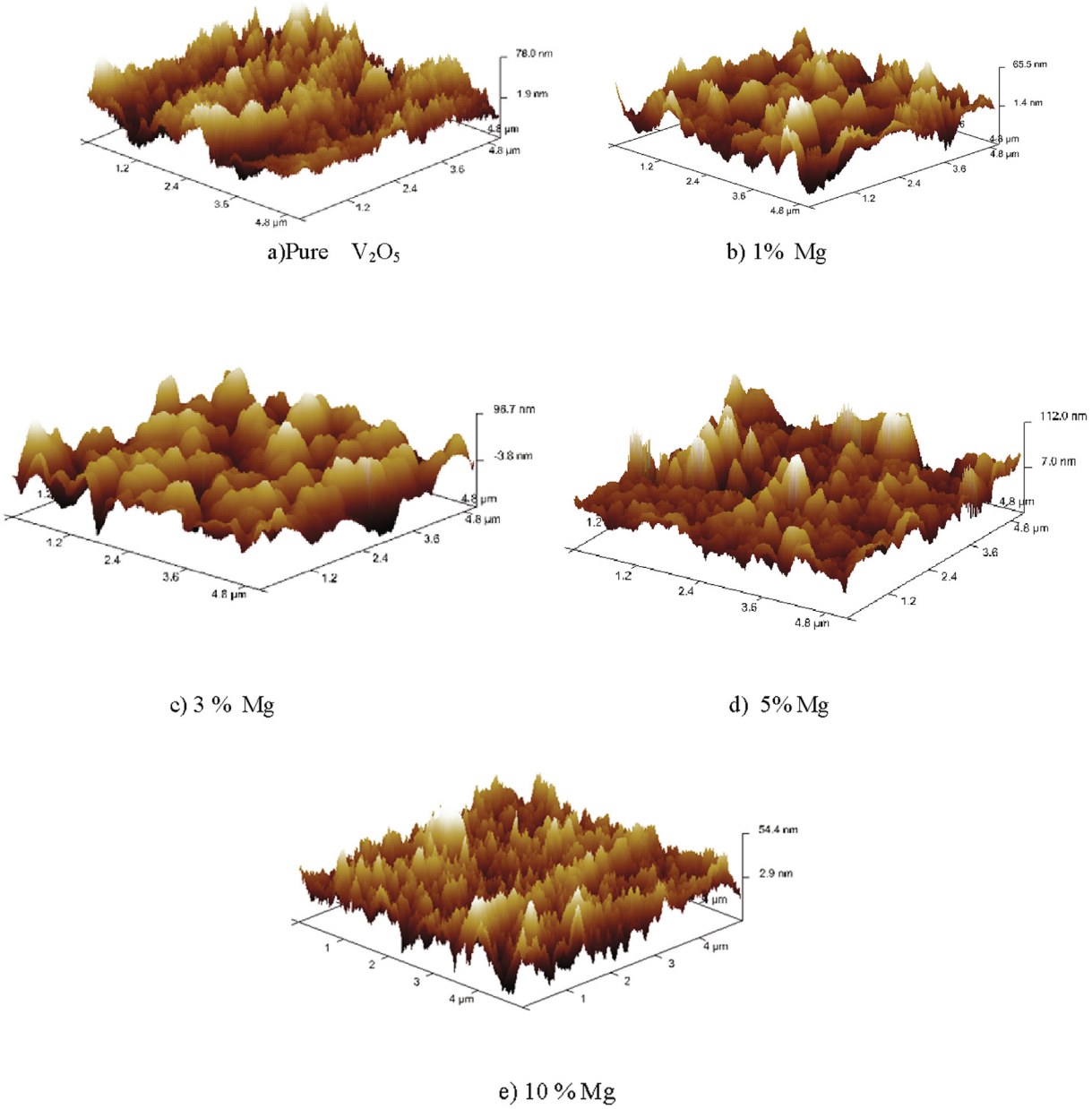

Fig. 6. AFM images of: a) pure V_2O_5, b) 1%, c) 3%, d) 5% and e) 10% Mg-doped V_2O_5 thin films.

3.4. Atomic force microscopy (AFM) image study

AFM images (Fig. 6) reveal that the surface roughness was increased from 54.4 nm to 112 nm with Mg-doping and is as shown in 3D images. The high surface roughness is mainly due to the 'O' vacancy present in the films. The sharp grain shapes of pure V_2O_5 changes to smooth grain size, which indicate the doping effect of Mg.

4. Conclusions

The thin-film fabrication using spray pyrolysis method is found to be simple and cost-effective for V_2O_5 thin films. The effect of Mg doping found to affect the structural, morphological and linear optical properties of V_2O_5 thin films. The XRD shows with poly-crystalline and an excellent crystalline behaviour with an orthorhombic phase which were grown preferentially along (200) plane. FESEM images confirm the non-homogeneous compared to the doped ones, which are also supported by the values of surface roughness. EDAX spectrum reveals the elemental composition of the prepared films found with predicted elements. The surface roughness has been increased with the Mg-doping. The bandgap energy was determined for the V_2O_5 films and found to be varied for about 2 wt% with the Mg-doping. The inspiring results with enhanced surface roughness suggest that the prepared Mg-doped V_2O_5 films are suitable and useful for optoelectronic, energy and gas-sensing applications.

Declaration of Competing Interest

The authors declare that they have no known competing financial interests or personal relationships that could have appeared to influence the work reported in this paper.

Acknowledgements

The author Sandesh Kumar Rai would like to acknowledge the provision of research facilities and study support by NMAMIT Nitte, India. Authors are also grateful to Mangalore University–India--DST-PURSE laboratory for FESEM facilities and MIT, Manipal, India for AFM facilities.

References

[1] H.S. Nalwa (Ed.), Encyclopedia of Nanoscience and Nanotechnology, American Scientific Publishers, Los Angeles, USA, 2004.
[2] A. Umar (Ed.), Encyclopedia of Semiconductor Nanotechnology, American Scientific Publishers, Los Angeles, USA, 2017.
[3] D. Wang, J. Yuan, Y. Zhou, H. Li, L. Chen, C. Song, Sci. Adv. Mater. 9 (2017) 2096.
[4] R. Singh, E. Singh, H.S. Nalwa, RSC Adv. 7 (2017) 48597.
[5] T. Kudo, Y. Ikeda, T. Watanabe, M. Hibino, M. Miyayama, H. Abe, K. Kajita, Sol. State Ionics 152 (2002) 833.
[6] A. Legrouri, T. Baird, J.R. Fryer, J. Catal. 140 (1993) 173.
[7] G.T. Kim, J. Muster, V. Krstic, J.G. Park, Y.W. Park, S. Roth, M. Burghard, Appl. Phys. Lett. 76 (2000) 1875.
[8] Q. Zhang, Q. Zhou, X. Yin, H. Liu, L. Xu, W. Tan, C. Tang, Sci. Adv. Mater. 9 (2017) 1350–1355.
[9] H. Song, C. Zhang, Y. Liu, C. Liu, X. Nan, G. Cao, J. Power Sources 294 (2015) 17.
[10] G.P. Patil, V.S. Bagal, M.A. More, D.S. Joag, N.S. Gajbhiye, K. Dewangan, P.G. Chavan, J. Nanoelectron. Optoelectron. 12 (2017) 286.
[11] Ji, D. Liu, C. Zhang, L. Yang, H. Cheng, and W. Zheng, 9, 861-867 (2017).
[12] A.E. Bulgurcuoglu, F.P. Gökdemir, O. Özdemir, K. Kutlu, J. Nanoelectron. Optoelectron. 12 (2017) 146.
[13] Y. Tang, A. Tang, J. Ouyang, Y. Zhang, Mater. Focus 6 (2017) 501.
[14] S. Ebrahimiasl, R. Seifi, R.E. Nahli, A. Zakaria, Sci. Adv. Mater. 9 (2017) 2045.
[15] V.B. Chanshetty, K. Sangshetty, G. Sharanappa, V. Dhanalakshmi, R. Anbarasan, Int. J. Eng. Res. Appl. 2 (2012) 611.
[16] E. Mauro, R. Díaz, C. Force, E. Comini, T. Andreu, R.R. Zamani, J. Arbiol, P. Siciliano, G. Faglia, J.R. Morante, J. Phys. Chem. C 117 (2013) 20697.
[17] G. Gu, M. Schmid, P.W. Chiu, A. Minett, J. Fraysse, G.T. Kim, S. Roth, M. Kozlov, E. Muñoz, R.H. Baughman, Nature Mater. 2 (2003) 316.
[18] N. Singh, A. Umar, N. Singh, H. Fouad, O.Y. Alothman, F.Z. Haque, Mater. Res. Bull. (2018).
[19] M. Panagopoulou, D. Vernardou, E. Koudoumas, N. Katsarakis, D. Tsoukalas, S. Yannis, Raptis J. Phys. Chem. C 121 (1) (2017) 70–79.
[20] K. Gurumurugan Devanesan Mangalaraj Sa.K. Narayandass Y. Nakanish, Materials Letters 28 (1996) 307-312.
[21] F. Gandarilla, A.A. Morales, O. Vigil, G.V. Hasiquio, L. Vaillant, P.V. Contreras, Mater. Chem. Phys. 78 (2003) 840–846.
[22] I. Ben Miled, M. Jlassi, I. Sta, M. Dhaouadi, M. Hajji, G. Mousdis, M. Kompitsas, H. Ezzaouia, J. Sol-Gel Sci. Technol. 83 (2017) 259–267.
[23] P.K. Ghosh, S. Das, K.K. Chattopadhyay, J. Nanopart. Res. 7 (2005) 219–2215.
[24] Charishma, A. Jayarama, V. Veena Devi Shastrimath, R. Pinto, Sahyadri, Int. J. Res. 3 (1) (2017) 37–46.
[25] Raghavendra Bairy, Parutagoudashankaragouda Patil, Shivaraj R. Maidur, H. Vijeth, M.S. Murari, Bhat K. Udaya, RSC Adv. 9 (39) (2019) 22302–22312.
[26] M. Abbasi, S.M. Rozati, R. Irani, S. Beke, Mater. Sci. Semiconductor Process. 29 (2015) 132–138.
[27] A.L. Patterson, Phys. Rev. 56 (1939) 978.
[28] C. Suryanarayana, M. Grant Norton (Eds.), X-Ray Diffraction, Springer US, Boston, MA, 1998.
[29] J. Tauc, Amorphous and Liquid Semiconductors, Plenum Press, New York, 1974, p. 159.